JOURNAL OF VIROLOGY, Jan. 1990, p. 195–206
0022-538X/90/010195-12$02.00/0

Vol. 64, No. 1

Mutations in VP1 of Poliovirus Specifically Affect Both Encapsidation and Release of Viral RNA

KARLA KIRKEGAARD

Department of Molecular, Cellular and Developmental Biology, University of Colorado, Boulder, Colorado 80309

Received 22 June 1989/Accepted 15 September 1989

The phenotypic defects of two type 1 Mahoney poliovirus mutants, termed VP1-101 and VP1-102, were caused by two different small deletions in the region of the RNA genome encoding the amino terminus of the capsid protein VP1. This portion of VP1 was unresolved in the three-dimensional structure of the poliovirion, buried within the virion, and likely to interact with the viral RNA. Both VP1-101 and VP1-102 showed a diminished ability to enter CV1 but not HeLa cells; both mutants formed plaques on CV1 and HeLa cells that were smaller than wild type. Neither the rate of binding to cells nor the rate of subsequent receptor-dependent conformational change of the mutant poliovirions was affected. However, both mutants displayed delayed kinetics of RNA release compared with wild-type virus. One of the mutants, VP1-102, also displayed a defect in viral morphogenesis: 75S empty capsids formed normally, but 150S particles that contained RNA accumulated much more slowly. We suggest that the VP1-102 mutation affects RNA encapsidation as well as RNA release, whereas the VP1-101 mutation affects only RNA release. Therefore, RNA packaging and RNA release are genetically linked but can be mutated separately in different VP1 alleles, and both processes involve the amino terminus of VP1.

The primary functions of viral capsids are to protect viral nucleic acids and to escort them into and out of host cells. The three-dimensional structure of the poliovirion has been determined by X-ray crystallography (17), providing insight into the way the virus might bind to its receptor and assemble in an infected cell. However, questions about function, such as how the poliovirus capsid allows the release of the viral RNA into the cell and how the capsid proteins assemble around the viral RNA to produce infectious stable virions, cannot be answered by understanding the structure alone. These questions can also be productively addressed by genetic and biochemical analysis of mutants defective in the processes of interest. Careful genetic analysis of poliovirus and certain other positive-strand RNA viruses is now possible due to the availability of infectious cDNA copies of the viral RNA genomes (31).

The construction and characterization of two Mahoney type 1 poliovirus mutants, VP1-101 and VP1-102, are reported in the accompanying paper (19). The mutations responsible for the phenotypic defects of these mutants are both small, in-frame deletions in the amino terminus of VP1. The phenotypes of these mutants include a reduction in the number of plaques formed on CV1 cells relative to that on HeLa cells and a diminution of plaque size on both cell types compared with wild-type poliovirus; these phenotypes are most apparent at 39.5°C (19). Here, I dissect the biochemical defects that are presumably responsible for the mutant phenotypes, with the goal of understanding the role of the amino-terminal sequences of VP1 in the function of the poliovirus capsid.

A poliovirus infection is initiated by the binding of the virion to the poliovirus receptor on the surface of the human or monkey cell. The human poliovirus receptor has recently been cloned, sequenced, and identified as a member of the immunoglobulin superfamily of cell surface molecules (25). The uptake of the virus into the cell subsequent to receptor binding is thought to occur by endocytosis of the virion-receptor complex, because infection by poliovirus (22) and other picornaviruses (28) is inhibited by chloroquine and ammonium chloride, agents that prevent vesicle acidification.

During cell entry, poliovirions undergo structural transitions in complex with the cellular receptors (34). The first such transition corresponds to a large conformational change: VP4, one of the capsid proteins, is lost; the altered particle displays a decreased sedimentation rate and increased protease sensitivity (12); and the viral RNA becomes sensitive to RNase A in the presence of sodium dodecyl sulfate (SDS) (16). If such altered poliovirions are recovered from the cell that they are in the process of infecting, they are uninfectious (18). The molecular details of this conformational change are not known, but it is a step that appears to be on the pathway to productive infection for all picornaviruses (10). Virion alteration has been shown to occur in cell-free membrane fractions (16, 18) and is similar to the structural transition that occurs during inactivation of poliovirions with heat or alkali (10).

Several antiviral compounds, including arildone (7, 24), rhodanine (13), WIN 51711 (41), and Ro 09-0410 (29), have been reported to block picornavirus infection by blocking viral "uncoating" or "eclipse," steps which correspond to the conformational change described above for poliovirus that results in the loss of VP4 and virion infectivity. The three-dimensional structure of human rhinovirus 14, another picornavirus, has been determined by X-ray crystallography in the presence (2, 37) and absence (33) of several such antiviral compounds. The inhibitors bind to the viral capsid and occupy a "pore" directly beneath an indentation encircling the five-fold symmetry axis of the icosahedral virion that is thought to be the binding site (9, 33) for ICAM-1, the major rhinovirus receptor (15, 38). The antiviral compounds have been proposed to act by making the picornavirus structures more rigid, increasing viral stability and preventing the conformational changes that are required for successful entry into target cells (2, 37).

Release of the viral RNA into the cell occurs subsequent to this conformational change. At this step, the viral RNA becomes RNase A sensitive even in the absence of SDS (16),

and virions that have matured in the presence of photoreactive dyes become light insensitive (40). Actually, the loss of light sensitivity of dye-containing virus particles, while thought to be correlated with RNA release, could coincide either with the physical release of the RNA or with a structural transition allowing the viral particle to become freely permeable to solvent (10, 22), an ambiguity addressed by the findings presented here.

After a poliovirus infection is initiated, new viral RNA and proteins accumulate. Although subviral particles of various sizes, as well as newly synthesized infectious virions, can be observed within the infected cell, the actual pathway of viral assembly has not been clarified. Probable scenarios describe 5S particles, which contain one copy each of VP0, VP1, and VP3, associating to form 14S particles or "pentamers," which contain five copies each of VP0, VP1, and VP3. These 14S particles may condense around the viral RNA directly or assemble first into 75S icosahedral "empty capsids" or "procapsids," containing 60 copies each of VP0, VP1, and VP3. A morphogenesis pathway that involves the 75S particles directly must then include a step in which the RNA threads into the empty capsid (34). In any case, 75S particles are found in infected cells, can be assembled in vitro from 14S subunits (30), and at least reflect the intrinsic self-assembling properties of the 14S particles (3). A particle whose reported sedimentation rate has ranged from 125S to 150S, termed the provirion, is thought to contain one copy of the 7,500-nucleotide viral RNA and 60 copies each of VP0, VP1, and VP3. Autoproteolytic cleavage of VP0 to the final products VP2 and VP4 would then be required to convert provirions into infectious 150S virions (1, 17, 33, 34).

The completed poliovirions consist of 60 copies each of VP1, VP2, VP3, and VP4 and one copy of the 7,500-nucleotide viral RNA and are resistant to a variety of treatments, including SDS, RNase, and low pH. Only a small percentage of the SDS-resistant 150S particles isolated from infected cells are infectious, however; the particle/PFU ratio for poliovirus can be in the thousands (10, 23, 34). Due to the large proportion of uninfectious virions present in any virion preparation, interpretation of the results of any biochemical experiments performed on a virion population is subject to the assumption that the biochemical properties of the infectious subpopulation are accurately represented. For this reason, I have chosen to analyze the VP1 mutant defects primarily by assays that measure only the infectious population.

As discussed in the accompanying paper (19), the deletion responsible for the phenotype of VP1-101 removes amino acids 8 and 9 from VP1, and the deletion of amino acids 1 to 4 from VP1 causes the VP1-102 phenotype. Even though the glutamine-glycine cleavage site for the viral 3C protease is altered in VP2-102, proteolytic processing appears to be normal (19). The drawing in Fig. 1 shows the amino acid backbone of VP1 and its orientation with respect to one of the five-fold symmetry axes of the icosahedral virion. The arrow denotes the amino terminus of VP1 as it projects into the interior of the particle (17). Analysis of the defects in these two mutants may delineate the wild-type functions of these sequences. It is shown here that both RNA packaging and RNA release can be affected by mutation of the amino terminus of VP1.

MATERIALS AND METHODS

Cells and viruses. Cell lines and growth conditions were as described in the accompanying report (19). Wild-type, VP1-101, VP1-102, and 3NC-202 virus stocks were all amplified from single plaques derived from transfection of the corresponding cDNAs: pPolio, pVP1-101, pVP1-102 (19), and p3NC-202, originally termed pPTH7387 (35). Plaque assays were performed as described; incubations were at 39.5°C for 44 h unless otherwise indicated. The titers of the virus stocks were defined as the titers at 39.5°C on HeLa cells, except for 3NC-202, whose titer was defined by its titer at 32.5°C. Multiplicities of infection (MOIs) were determined by using the titer of wild type, VP1-101, and VP1-102 at 39.5°C on HeLa cells.

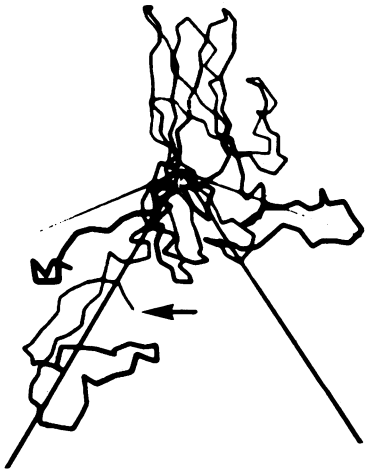

FIG. 1. Diagram of the peptide backbone of poliovirus capsid protein VP1 and its arrangement at the fivefold symmetry axis of the icosahedral virion. The arrow denotes the most amino-terminal residue of VP1 resolved in the three-dimensional structure determined to 2.9 A resolution. (From Hogle et al. [17]; used with permission.)

Infectious-center assays, in which plaque assays were initiated with infected cells, were begun by infecting either HeLa or CV1 cell monolayers in 100 mm petri dishes (Corning) with virus at MOIs of 0.01 to 0.1 PFU/cell. Viruses were allowed to bind to the cells for 30 min at 39.5°C for wild type, VP1-101, and VP1-102 or at 32.5°C for 3NC-202 virus. The monolayers were then washed twice with phosphate-buffered saline (PBS); 10 ml of Dulbecco modified Eagle medium (DME) supplemented with 10% fetal calf serum (GIBCO) was added to each plate, and incubation was continued for 90 min. Subsequently, the medium was removed and the cells were dislodged from the petri dishes with 1 ml of a 0.4% trypsin solution (Irvine Scientific). Ten milliliters of DME supplemented with 10% calf serum (GIBCO) was added to the trypsin mixture. The cells were sedimented by centrifugation at 800 × *g* for 5 min and resuspended in 5 ml of DME with 10% calf serum. Four sequential 10-fold dilutions of the cells were made in DME with 10% calf serum, and 0.5 ml of each dilution was added directly to HeLa and CV1 cell monolayers in 100-ml petri dishes. Agar overlays containing 0.9% Bacto-agar (Difco Laboratories), DME, and 10% calf serum were added immediately. Wild-type, VP1-101, and VP1-102 plates were incubated at 39.5°C for 44 h; 3NC-202 plates were incubated at 32.5°C for 72 h. After removal of the agar overlay, plates were stained with crystal violet as described before (6).

DNA plasmids and RNA transfections. Plasmid pT7D (35), in which the full-length poliovirus cDNA is located downstream of a T7 RNA polymerase promoter, was kindly provided by P. Sarnow (University of Colorado Health

Sciences Center). This plasmid directs the transcription of full-length poliovirus RNA differing in sequence from virion RNA only by the presence of two guanosine residues at the 5′ end and by encoding a poly(A) tract only 12 nucleotides long. Plasmids T7VP1-101 and T7VP1-102 were constructed by replacing the Pflm 1 DNA fragment, nucleotides 496 to 3625 of the poliovirus cDNA (20, 32), in T7-polio with the corresponding fragment from pVP1-101 and pVP1-102, respectively. Digestion of the plasmids with *Mlu*I, T7 transcription, and DEAE transfection were all performed as described by Sarnow (35).

Measurement of virus-specific RNA synthesis and single-cycle infections. The amount of [^{3}H]uridine incorporated during poliovirus infection of CV1 and HeLa cells in the presence of dactinomycin was determined as described by Bernstein et al. (6). In the time courses of virus-specific RNA synthesis for the wild type, VP1-101, and VP1-102, time zero was defined as the time postabsorption at which the dactinomycin-containing medium and [^{3}H]uridine were added. The background [^{3}H]uridine incorporation in mock-infected cells after 6 h of incubation was approximately 4,000 cpm for both CV1 and HeLa cells.

For complementation and interference experiments, appropriate amounts of each virus or combination of viruses were bound to duplicate 60-mm dishes containing HeLa cell monolayers for 30 min at 39.5°C, after which the monolayers were washed twice with PBS. Five milliliters of DME containing 10% calf serum was added, incubation was continued for 4 or 5 h at 39.5°C as indicated, and the cells were washed with PBS and scraped into 1 ml of PBS. The solutions were frozen and thawed twice, the cell nuclei were pelleted by centrifugation at 1,600 × *g* for 10 min at 4°C, and the resulting cytoplasmic extracts were used as virus stocks for subsequent plaque assay. The identities of the plaques resulting from infection with different viruses were readily identifiable by plaque phenotype, as were wild-type recombinants.

Binding assays. To determine the percentage of particles bound in 30 min at 39.5°C, ^{3}H-labeled virions were absorbed to HeLa and CV1 cell monolayers in 0.5 ml of PBS. The amount of radioactivity remaining bound to the cells after extensive washing with PBS and the starting amount of radioactivity in the inoculum were determined by scintillation counting of nitrocellulose filters after trichloroacetic acid precipitation and filtering of the labeled particles. ^{3}H-labeled virions were prepared by infecting approximately 10^8 HeLa cells (as monolayers in five 150-mm petri dishes each) with wild-type, VP1-101, and VP1-102 viruses at MOIs of 50. After absorption, 10 ml of DME with 10% calf serum and 30 μCi of [^{3}H]uridine per ml were added to each plate. Incubations at 37°C were continued until cytopathic effects were marked, at which time the cells were harvested by scraping. Virions were isolated by equilibrium centrifugation in CsCl density gradients by standard methods (4, 5) and dialyzed into PBS.

To determine the percentage of virions that bound and remained infectious in 30 min at 39.5°C or in 60 min at 4°C, viruses were bound to CV1 or HeLa cells at MOIs of 50 in 0.5 ml of PBS, followed by extensive washing with room-temperature PBS. Viruses were released and harvested by freezing and thawing the collected cells and preparing cytoplasmic extracts.

Conformational alteration and RNA release assays. For alteration assays, wild-type, VP1-101 and VP1-102 viruses were prebound to HeLa and CV1 monolayers at 4°C for 60 min at MOIs of 0.1 PFU/cell. The monolayers were washed three times with room-temperature PBS, and 0.5 ml of PBS was added to each 60-mm petri dish to prevent the cells from drying during subsequent incubation at 39.5°C for various time periods. After incubation, an additional 0.5 ml of PBS was added to each plate, the cells were harvested by scraping, and cytoplasmic extracts were prepared and titered by plaque assay on HeLa cells.

Neutral red-containing virus was prepared for the RNA release assays by harvesting wild-type, VP1-101, and VP1-102 virus from HeLa monolayers grown in the presence of 10 μg of neutral red (Aldrich) per ml as described before (11, 40). Cytoplasmic extracts were prepared and used as virus stocks. During virus growth, the plates were wrapped in velvet, and all manipulations were performed under low levels of red light. To determine the optimal time of irradiation to inactivate the NR viruses with an available white light source (American Medical Sales model 201, 40 W), 200 PFU of each NR virus was absorbed onto each of several HeLa monolayers, the cells were washed with PBS, an agar overlay was applied, and the plates were irradiated immediately by direct placement on the light box for various periods of time. An optimal time of irradiation, 8 min, was found, during which 95% of each of the NR viruses was inactivated (data not shown).

Time courses of RNA release were determined by prebinding approximately 200 PFU of each virus to monolayers of CV1 and HeLa cells in 60-mm dishes at 4°C for 60 min. The monolayers were washed twice with room-temperature PBS, agar overlays were added immediately, and duplicate plates were irradiated for 8 min after various times of incubation at 39.5°C. Control plaque assays of the NR viruses, which received no irradiation, were done in parallel. The data were quantified by counting the numbers of plaques on the irradiated plates, and these values were expressed as a percentage of the number of plaques on the unirradiated control.

Analysis of viral and subviral particles. To allow the incorporation of [^{35}S]methionine into virus-specific particles, HeLa and CV1 cells in 100-mm petri dishes were injected with viruses and incubated at 39.5°C in DME with 10% calf serum. MOIs for wild-type, VP1-101, and VP1-102 viruses were all 20 PFU/cell on HeLa cells and 100, 500, and 500 PFU/cell, respectively, on CV1 cells. The increased nominal MOIs on CV1 cells were used to bypass the cell entry defects of all the viruses on CV1 cells. After 3 h of incubation, the cells were washed with DME lacking methionine (GIBCO), 2.0 ml of DME lacking methionine, containing 50 μCi of [^{35}S]methionine (ICN) per ml was added to each plate, and incubation at 39.5°C was continued for either 30 or 90 min. Cells were washed and harvested by scraping into 1 ml of a solution containing 10 mM Tris (pH 7.4), 10 mM NaCl, 1.5 mM $MgCl_2$, 1% Nonidet P-40, 1 μM phenylmethylsulfonyl fluoride (Sigma), and 40 U of placental RNasin (Promega) per ml. Nuclei were pelleted by centrifugation at 1,600 × *g* for 10 min at 4°C, and 0.5 ml of the resulting cytoplasmic extract was loaded directly on 11-ml gradients containing 15 to 30% sucrose in 10 mM Tris (pH 7.4)–10 mM NaCl–1.5 mM $MgCl_2$. The particles were sedimented through the sucrose gradients by centrifugation for 3 h at 27,500 rpm at 15°C, with a Beckman SW41 rotor. The gradients were analyzed by collecting 0.5-ml fractions; 2 ml of 10% trichloroacetic acid was added to 0.2 ml of each fraction, the precipitate was collected by filtration through nitrocellulose, and the radioactivity bound to each filter was determined by scintillation counting. The 150S and 75S peaks were identified by correlation with published values

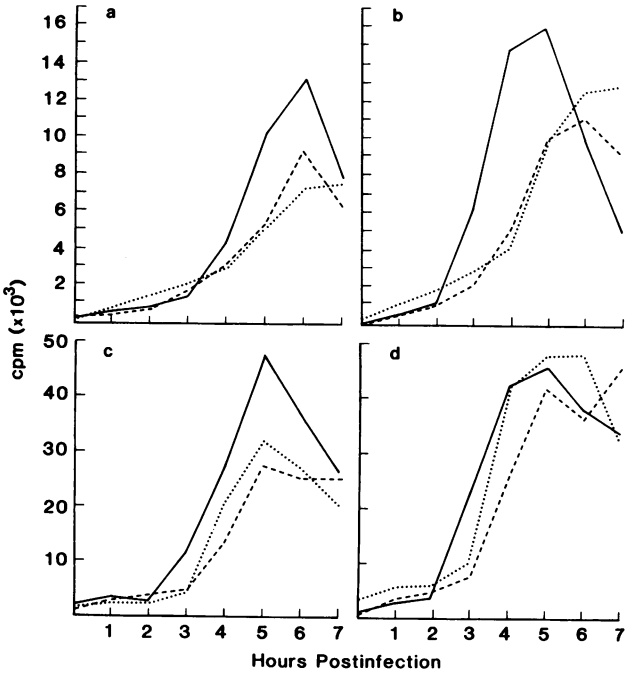

FIG. 2. Wild-type (——), VP1-101 (– – –), and VP1-102 (· · · · ·) virus-specific RNA synthesis in CV1 and HeLa cells. (a) [³H]uridine incorporation in CV1 cells at MOIs of 10 for each virus. (b) [³H]uridine incorporation in CV1 cells at MOIs of 200 for each virus. (c) Virus-specific RNA synthesis in HeLa cells infected with each virus at an MOI of 10. (d) Virus-specific RNA synthesis in HeLa cells infected with each virus at an MOI of 200.

and their predicted behavior (34) in response to treatments with SDS and EDTA (data not shown).

RESULTS

VP1-101 and VP1-102 RNA synthesis shows increased dependence on MOI. Virus-specific RNA synthesis in CV1 and HeLa cells infected with wild-type, VP1-101, and VP1-102 poliovirus at different MOIs is shown in Fig. 2. At a low MOI of 10 PFU/cell, viral RNA synthesis in CV1 cells infected with VP1-101 and VP1-102 clearly occurred but at lower levels than that of wild-type virus at the same MOI (Fig. 2a). Figure 2b, in which the MOIs of both wild-type and mutant viruses were 200 PFU/cell, shows an increase in virus-specific RNA synthesis for all the viruses. Increased MOI can both increase the amount of viral RNA produced in a single-cycle infection and diminish the time lag before maximal RNA synthesis begins (4). Both of these effects were seen in the wild-type infection of CV1 cells in Fig. 2b, but RNA synthesis for both mutants was still not maximal. In fact, the mutant viral RNA curves for Fig. 2b, determined at an MOI of 200, were nearly superimposable with the wild-type curve in Fig. 2a, done at an MOI of 10.

Parallel experiments on HeLa cells (Fig. 2c and d) revealed a similar pattern. At MOIs of 10 PFU/cell, mutant virus-specific RNA synthesis was depressed relative to that of wild-type virus. At an MOI of 200 PFU/cell on HeLa cells (Fig. 2d), both wild-type and VP1-101 viruses showed an increase in the amount of RNA synthesis and a decrease in the lag time before maximal RNA synthesis began. VP1-102 RNA synthesis was only slightly lower at this high MOI on HeLa cells than in the other two viruses.

Thus, both mutants VP1-101 and VP1-102 can synthesize viral RNA. However, the levels of RNA synthesis are more MOI dependent than those of wild-type virus. These findings suggest that the diminished levels of RNA synthesis in the mutants are not a primary effect of the mutations, but an effect secondary to the apparent MOI.

Plaque reduction phenotypes of VP1-101 and VP1-102 can be overcome in infectious-center or RNA transfection experiments. Wild-type Mahoney serotype 1 poliovirus formed fewer plaques on CV1 than on HeLa cells (Fig. 3). The ratio of the numbers of plaques formed on HeLa to CV1 cells varied with the experimental conditions, but was usually from 6 to 15. All experiments were performed at 39.5°C, the

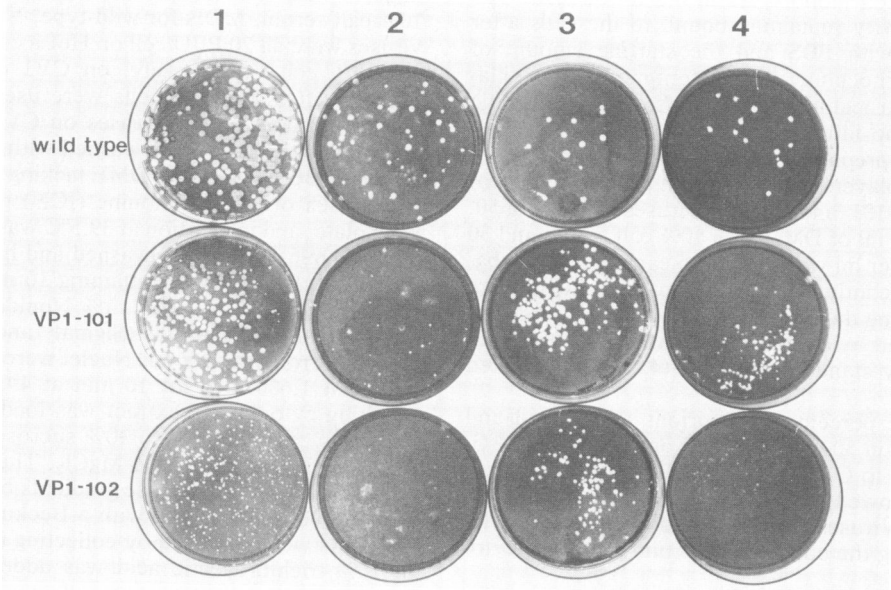

FIG. 3. Plaque assays and infectious-center assays of wild-type, VP1-101, and VP1-102 viruses on HeLa (columns 1 and 3) and CV1 (columns 2 and 4) cells. Columns 1 and 2 show plaque assays of all three viruses at identical dilutions on HeLa and CV1 cells. Columns 3 and 4 display the results of infectious-center assays on HeLa and CV1 cells, in which plaque formation was initiated by infected CV1 cells as described in Materials and Methods.

TABLE 1. Ratios of plaques formed on HeLa cells to those formed on CV1 cells following infection and transfection

Virus	HeLa/CV1 plaque ratio in infection initiated with:		
	Virions	Infected cells[a]	RNA[a]
Wild type	7	1.4	6.4
		1.5	5.7
VP1-101	36	1.3	5.8
		0.9	14.7
VP1-102	98	1.3	8.1
		1.4	2.9

[a] Results of duplicate experiments are shown.

condition under which the mutant phenotypes were most pronounced (19). Both VP1-101 and VP1-102 viruses formed even fewer plaques on CV1 cells than on HeLa cells. In a number of experiments, the HeLa/CV1 ratios of these mutants both ranged from 35 to 120, but were always 5- to 10-fold greater than the wild-type ratio in any given experiment. One such experiment is presented in Table 1. Perhaps a more striking aspect of the phenotypes of VP1-101 and VP1-102 is their formation of small plaques on HeLa cells (Fig. 3, column 1) and very small plaques on CV1 cells (Fig. 3, column 2). However, the plaque reduction aspect of both their phenotypes proved useful in demonstrating a primary defect for both mutants in cell entry.

If the reduction in the number of plaques formed by VP1-101 or VP1-102 is caused by a defect in cell entry or some other early, MOI-dependent defect, the plaque reduction phenotype should disappear when plaque formation is initiated by an infected cell instead of a viral particle. In such an infectious-center assay, the infected cell, when it lyses, will inoculate its neighbors with high doses of infectious particles, and the MOI-sensitive step in plaque formation will have been bypassed.

In Fig. 3, plates are shown on which wild type, VP1-101, and VP1-102 infections were initiated with either virus particles (columns 1 and 2) or infected CV1 cells (columns 3 and 4). It is apparent that the discrepancy in the numbers of plaques formed by wild-type, VP1-101, and VP1-102 virions on HeLa and CV1 cells disappeared in infectious-center assays; these ratios are given in Table 1. Identical results were obtained whether the infectious centers were prepared from infected HeLa or CV1 cells. Not all mutant phenotypes can be masked when plaque assays are initiated with previously infected cells, In infectious-center assays performed with a poliovirus mutant defective in RNA replication, the temperature-sensitive mutant 3NC-202 (36), the temperature-sensitive phenotype was completely reproduced (data not shown). Furthermore, as shown in Fig. 3, the small-plaque phenotypes of both VP1-101 and VP1-102 were still evident in the infectious-center assays.

Apparently, an early, MOI-dependent defect is responsible for the plaque reduction of both VP1-101 and VP1-102 virions on CV1 cells. This conclusion is also consistent with the MOI dependence of the RNA synthesis data (Fig. 2). That the same or another defect continues to be limiting in the propagation of the mutant plaques is shown by the persistence of the small-plaque phenotypes of both mutants on both HeLa and CV1 cells. The reduced ability of wild-type virus to form plaques on CV1 cells was also abolished when the infection was initiated with infected cells; therefore, even wild-type poliovirus displays an early, MOI-dependent defect in initiating an infection in CV1 cells relative to the ability of wild-type virus to infect HeLa cells.

If the diminished numbers of CV1 plaques formed by VP1-101 and VP1-102 result from the mutant capsid proteins' causing a defect in the ability of the viruses to enter cells, then initiating the plaque assays with RNA instead of virions should also overcome the plaque reduction phenotype. Infectious wild-type, VP1-101, and VP1-102 RNA was synthesized in vitro by T7 RNA polymerase transcription of DNA plasmids (35, 39) containing the cDNA sequences of the three viruses and a T7 promoter (Materials and Methods). These RNA molecules were transfected into HeLa and CV1 cells. From the ratios of the numbers of plaques formed on HeLa cells to the numbers formed on CV1 cells given in Table 1, it is apparent that initiating an infection by RNA transfection also eliminated the differences between mutant and wild-type infections in plaque-forming efficiency on HeLa and CV1 cells. The transfection and plaque-forming efficiencies of even wild-type RNA were greater on HeLa than on CV1 cells, and a certain amount of variability in the experiments can be seen in Table 1. However, any differences observed in the HeLa/CV1 ratios are not sufficient to explain the mutant phenotypes. In addition, the plaques formed following transfection of VP1-101 and VP1-102 RNA retained the small-plaque phenotypes characteristic of each mutant on both cell lines (data not shown). Thus, subsequent propagation of the plaques was still affected by the mutations to various extents, even when the infections were initiated with RNA or infected cells.

Some feature of the mutated viruses renders initiation of plaque formation rate-limiting, especially on CV1 cells at 39.5°C. To test the idea that VP1-101 and VP1-102 viruses are defective in entering cells and to determine at which point the defects occur, the behavior of the mutants in the different steps of entry into HeLa and CV1 cells was studied and compared with that of wild-type virus.

Initial binding of VP1-101 and VP1-102 to HeLa and CV1 cells is comparable to that of wild-type virus. The most straightforward way to measure the binding of viruses to cells is to prepare radioactive virions, expose them to cells for a certain length of time, wash the cells extensively, and determine the amount of radioactivity bound to the cells. The results of such an experiment are shown in Table 2. After incubation with cells for 30 min at 39.5°C, similar to the usual plaque assay conditions, similar percentages of each preparation of labeled particles were bound to each cell line. The HeLa/CV1 ratios of the amounts of ^{3}H-labeled particles bound to the two different cell lines were also comparable for the different viruses. A possible reduction in the HeLa/CV1 ratio observed for the VP1-102 particles did not appear to be significant.

Interpretation of the preceding binding results required the assumption that the population of viral particles reflected the biochemical behavior of the subpopulation of particles that were actually infectious. Furthermore, the relative size of this infectious subpopulation was found to vary between different viruses and different preparations of the same virus. For example, in the preceding experiment, wild-type, VP1-101, and VP1-102 virions were prepared following growth conditions in which [^{3}H]uridine was present at identical concentrations in the medium for all the infections. The specific activities of the resulting ^{3}H-labeled virus particles were 8×10^{-6}, 8×10^{-5}, and 4×10^{-5} cpm/PFU for wild-type, VP1-101, and VP1-102 viruses, respectively. That is, the particle/PFU ratios differed substantially, with the percentage of wild-type particles that were infectious being higher than that of either of the mutant populations. This is probably a significant aspect of the mutant phenotypes, but

TABLE 2. Binding of wild-type and mutant viruses to HeLa and CV1 cells

Virus	% of cpm bound[a]			% of PFU bound[b]			% of PFU bound[c]		
	HeLa	CV1	HeLa/CV1	HeLa	CV1	HeLa/CV1	HeLa	CV1	HeLa/CV1
Wild type	13	12	0.97	1.5	0.62	2.7	4.9	1.9	2.8
	15	17		1.4	0.46		5.7	1.9	
VP1-101	13	10	0.96	2.7	0.91	2.4	3.3	1.1	3.0
	14	14		2.4	1.2				
VP1-102	7.9	14	0.78	2.0	0.92	1.9	3.4	1.3	2.6
	17	18		2.0	1.2				

[a] Cells were exposed to all viruses at MOIs of 100 to 500 PFU/cell. After virus binding to cells at 39.5°C for 30 min, the extent of ^{3}H-labeled virus binding in duplicate experiments was determined by scintillation counting. The HeLa/CV1 ratio is the average of the data shown.

[b] After binding to HeLa or CV1 cells at 39.5°C for 30 min as above, viruses were eluted and counted on HeLa cells as described in Materials and Methods.

[c] Mutant and wild-type viruses were bound to HeLa and CV1 cells at 4°C for 60 min. Bound virus was assayed as described above.

could further confound an experiment in which the direct binding of all viral particles was measured.

Another way to measure the binding of viruses to cells is to elute them from the cells subsequent to binding and to count the infectious particles that can be recovered. The results of such experiments are shown in Table 2. Again, neither the percentages of wild-type, VP1-101, or VP1-102 PFU that bound to the cells nor the HeLa/CV1 ratios of those percentages differed significantly. The percentages of bound PFU were lower than the percentages of bound labeled particles for each virus. This probably resulted from the conformational alteration of those particles subsequent to binding (see next section). It is shown below, however, that conformational alteration of the mutant and wild-type virions proceeds at identical rates, so any differential effect of alteration on these results is excluded. Thus, the physical binding of VP1-101 and VP1-102 to HeLa and CV1 cells is unaffected by the mutations. Similar ratios of binding to CV1 and HeLa cells of infectious mutant and wild-type particles were also seen at 4°C (Table 2), at which temperature conformational alterations subsequent to binding do not occur.

Neither the rate nor the extent of viral alteration is changed in VP1-101 or VP1-102. Subsequent to binding to the viral receptor at the cell surface, conformational changes in the poliovirion ensue that have been termed alteration. Empirically, alteration has been correlated with numerous physical changes in virion structure, such as loss of VP4, increased RNase and protease sensitivity, and decreased sedimentation rate (10, 34). Here, loss of infectivity was used as an assay of alteration in order to measure only the infectious population of virions. Conformational change leading to loss of infectivity does not occur at lower temperatures (10). Populations of infecting viruses can therefore be synchronized by prebinding at 4°C. A temperature switch to 39.5°C then allows the bound virions to begin their postbinding processes simultaneously.

The results of such experiments are shown in Fig. 4. After prebinding at 4°C for 60 min, viruses bound to cells were recovered after various periods of incubation at 39.5°C. The titers of the resulting virus stocks were determined by plaque assay. The amount of infectious virus present after prebinding at 4°C, with no incubation at 39.5°C, was defined as 100% unaltered. Soon after incubation at 39.5°C began, the bound virions lost infectivity; more than half were altered after 15 min. The time courses in Fig. 4 display both the rates and extents of uncoating of wild type, VP1-101, and VP1-102 on CV1 and HeLa cells. No significant mutant-specific differences were seen on either cell line. Alteration of the viral particles seemed to proceed normally for both VP1-101 and VP1-102, and any defect in cell entry must occur later.

VP1-101 and VP1-102 display altered rates of RNA release on both CV1 and HeLa cells. RNA release, the step at which the viral RNA is released from the viral capsid, has been defined as the point at which the viral RNA becomes RNase sensitive in the absence of ionic detergent (16). In an attempt to measure the infectious population of viral particles directly, the loss of photosensitivity of virions grown in the presence of a chromogenic dye (11, 40) was monitored. For this assay, virus stocks were prepared in the presence of neutral red; the resulting NR virus was able to initiate an infection normally so long as it was kept in the dark. The period of light sensitivity has been correlated with the time required for the virus to release its RNA (10, 40). It is thought that, after RNA release, the reversibly bound dye molecules can diffuse away from the RNA with which they were encapsidated, and thus the RNA can no longer be destroyed by irradiation (10).

In Fig. 5, the results of experiments in which the escape of the viral RNA from copackaging with the neutral red dye molecules was monitored are shown. Wild-type, VP1-101, and VP1-102 viruses were prebound to monolayers of CV1 and HeLa cells at 4°C; the monolayers were then washed extensively and transferred to 39.5°C incubators for various periods of time. All manipulations were performed under low levels of red light as described before (40). Figure 5a shows the results of one such experiment. The first plates on the left show the results of infecting HeLa cells with NR–wild-type and NR–VP1-101 viruses with no irradiation; approximately 200 plaques formed on each plate. The second set of plates shows the result of irradiating the cells (Materials and Methods) before any incubation at 39.5°C; more than 95% of the infectious virus was inactivated. With increasing periods of incubation time at 39.5°C, increasing amounts of virus escaped inactivation; by 60 min, 100% of the wild-type virus was immune to irradiation. The amount of NR–VP1-101 virus, however, increased more slowly; the difference was seen most clearly at the 10- and 20-min time points. Furthermore, the total extent of escape of NR–VP1-101 viruses from irradiation sensitivity at the last time point was also lower than that of the wild-type virus.

These data are shown graphically in Fig. 5b and c. In both graphs, the number of plaques that formed with no irradiation at all is defined as 100%, and all other values are given as a percentage of this unirradiated-control value. On CV1 cells (Fig. 5b), a pronounced lag in the loss of sensitivity to irradiation was observed for both mutants, indicating that both VP1-101 and VP1-102 show a defect in RNA release under these conditions. The times at which 50% of the viruses had released their RNA, $t_{1/2}$, for wild type, VP1-101, and VP1-102 on CV1 cells were 17, 33, and 40 min, respectively.

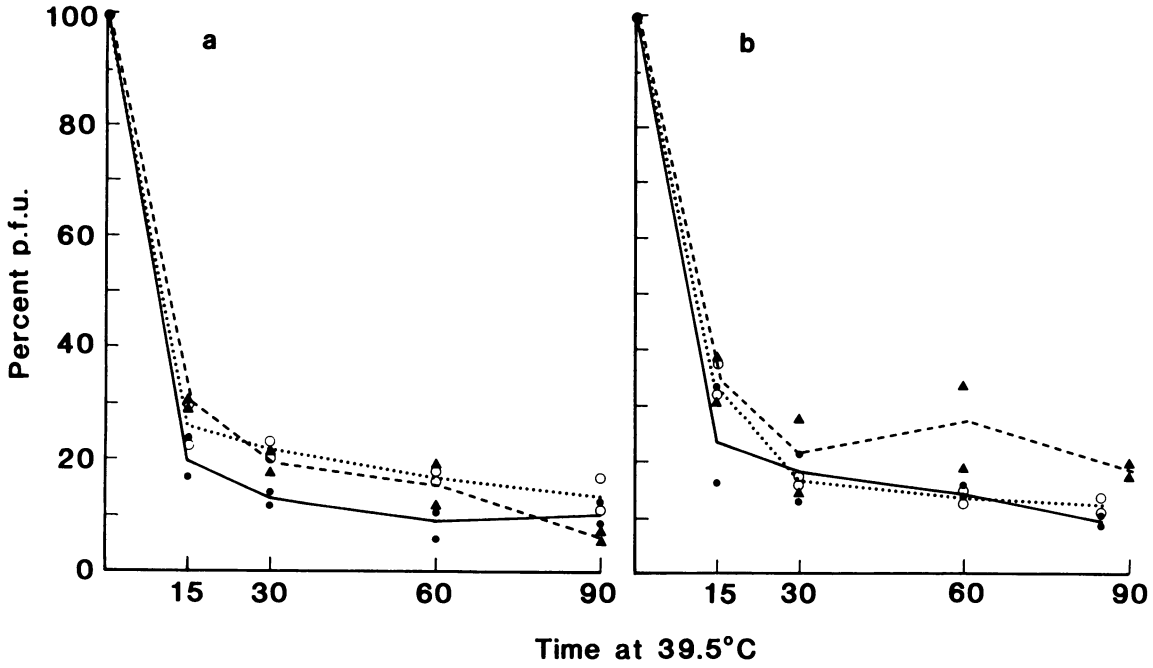

FIG. 4. Time courses of alteration of mutant and wild-type viruses on CV1 and HeLa cells. Viruses were adsorbed to cell monolayers at low temperature to allow binding but not subsequent changes; the number of infectious unaltered virions is shown as a function of time at 39.5°C after temperature shift. The amount of infectious virus before any 39.5°C incubation was defined as 100% unaltered for each experiment; other values are given as a percentage of this amount. The average values of duplicate points are connected for wild type (●; ——), VP1-101 (▲; – – –), and VP1-102 (○; · · · ·) viruses. (a) Time course of alteration for each virus on CV1 cells. (b) Similar data for each virus on HeLa cells.

The extent of RNA release after 60 min at 39.5°C was similar for all the viruses on CV1 cells. Neither the wild-type nor either of the mutant NR viruses completely unencapsidated their RNA within the time of the experiment; further time points may have revealed further RNA release on CV1 cells. Perhaps this effect is part of the reason for the reduced numbers of even wild-type plaques formed on CV1 cells.

The results of similar experiments with HeLa cells are shown in Fig. 5c. Again, both mutants showed a lag in RNA release relative to wild-type virus; the $t_{1/2}$s of RNA release for wild type, VP1-101, and VP1-102 were 18, 48, and 31 min, respectively. On HeLa cells, both wild-type and VP1-102 NR viruses appeared to unencapsidate their RNA completely within 60 min; both viruses approached the number of plaques in the unirradiated control with increased time of incubation at 39.5°C. NR–VP1-101 virus, however, did not; the significance of this observation is not clear at this time.

VP1-101 and VP1-102 thus show altered kinetics of RNA release at 39.5°C on both CV1 and HeLa cells. The phenotypes of these two mutants were originally defined as having both plaque reduction and small-plaque characteristics on CV1 cells. Why is there a defect in RNA release on both HeLa and CV1 cells? One possibility is that unencapsidation of viral RNA is a rate-limiting step in CV1 cells but not HeLa cells, and thus plaque formation in CV1 cells is much more sensitive to a defect in RNA release. A second possibility is that VP1-101 and VP1-102 are defective in cell entry and, specifically, in RNA release, on both cell lines, and that this effect is slightly more pronounced on CV1 cells. The increased particle/PFU ratio for both VP1-101 and VP1-102 on HeLa cells argues for the second suggestion.

VP1-102 shows an additional defect in RNA packaging. Growth curves in which the numbers of infectious particles of wild-type, VP1-101, and VP1-102 viruses were measured over the course of a single-cycle infection showed diminished yields of both mutant viruses (Tables 3 and 4; time course not shown). Even at MOIs sufficiently high to overcome the cell entry defects, the yield of VP1-101 virus was usually fivefold diminished, and the yield of VP1-102 virus 50-fold reduced relative to a wild-type infection on either CV1 or HeLa cells. The lower yield of VP1-101 could be the result of the increased percentage of defective particles produced; the reduction of VP1-102 titer, however, seemed too large to be explained in this way. An additional defect in the VP1-102 infectious cycle was therefore sought.

The largest of the viral and subviral particles accumulated during wild-type, VP1-101, and VP1-102 infections are shown in Fig. 6. The amounts and identities of the particles were monitored by sucrose gradient sedimentation of cytoplasmic extracts from viral infections performed in the presence of [^{35}S]methionine. Infectious virions sediment at 150S; empty capsids, or "procapsids," sediment at 75S. Empty capsids do not contain RNA and are expected to be in equilibrium, both in vivo and in vitro, with 14S pentamers (34). In this experiment, the extent of RNA encapsidation in a given infection was estimated from the amount of material in the 150S peak, and the relative amount of RNA-less subviral particles present in the infection was estimated from the amount of material in the 75S peak.

The tracings in Fig. 6a show the viral and subviral particle profiles from CV1 cells infected with wild-type, VP1-101, and VP1-102 viruses at high MOIs to overcome the cell entry defects of the mutants. [^{35}S]methionine was added to the medium 3.5 h post-infection, and labeling was continued for 30 min. The approximately 1:1 ratio of material in the 150S and 75S peaks in the wild-type infection was clearly changed for both mutants. Much less 150S material accumulated during the VP1-102 infection, suggesting that RNA packag-

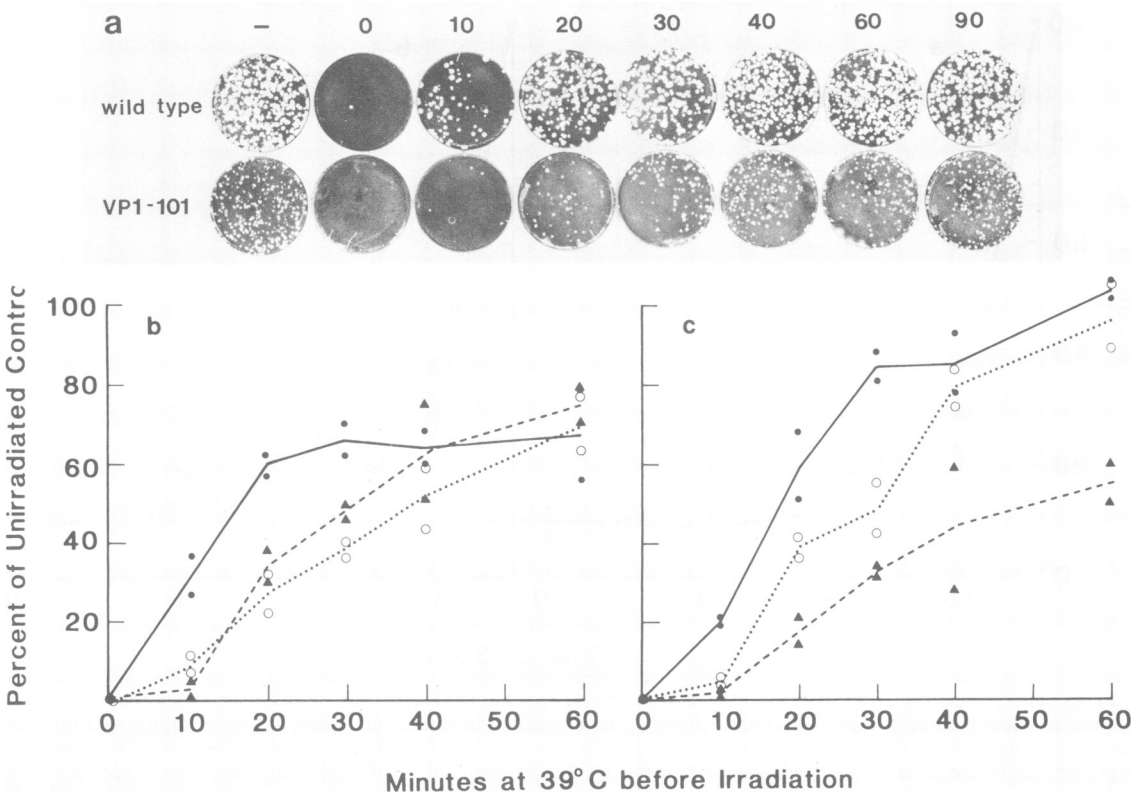

FIG. 5. Time course of RNA release of mutant and wild-type viruses on CV1 and HeLa cells. (a) Increase in resistance to irradiation of wild-type and VP1-101 NR viruses after the indicated time (in minutes) of incubation at 39.5°C or after incubation at 39.5°C with no irradiation at any time (column —). The time courses of RNA release of wild type (●; ——), VP1-101 (▲; – – –), and VP1-102 (○; · · · · ·) are shown graphically for CV1 cells (b) and HeLa cells (c). The averages of duplicate points for each virus are connected by the curves.

ing occurred more slowly. Surprisingly, a larger amount of 150S material accumulated relative to the 75S peak in the VP1-101 infection; this effect was only somewhat reproducible, but may represent a slightly increased rate of RNA packaging in VP1-101.

TABLE 3. Complementation in single-cycle infections

Infection no.	Virus(es)	MOI (PFU/cell)	Titer[a] after 4 h at 39.5°C (10^6 PFU/ml)	HeLa/CV1 plaque ratio[b]
1	3NC-202	100	0.0095 0.0025	14
2	Wild type	10	2,250 2,100	14
3	Wild type, 3NC-202	10, 100	2,200 1,500	11
4	VP1-101	10	355 450	106
5	VP1-101, 3NC-202	10, 100	635 640	43[c]
6	VP1-102	10	48 83	102
7	VP1-102, 3NC-202	10, 100	56 69	—[d]

[a] Results of duplicate experiments are shown.
[b] Average of duplicate experiments is given.
[c] The apparent increase in titer on CV1 cells was not due to the presence of recombinant viruses in the mixed infection. Recombinant viruses could be clearly distinguished by plaque morphology and were not prevalent enough to account for the observed effect.
[d] The presence of recombinant viruses in the progeny of the mixed infection made determination of this value difficult.

The same experiment is shown in Fig. 6b, but the labeling with [^{35}S]methionine was continued for 90 min. Again, the 150S peak was greatly reduced in the VP1-102 infection relative to either the wild-type or VP1-101 infections of CV1 cells. VP1-102 virion or provirion particles were formed, but apparently at a greatly diminished rate.

The viral and subviral particles made during a 90-min labeling of HeLa cells are shown in Fig. 6c. The relative abundance of the 150S peak was again lower for the VP1-102 infection, although the effect was less dramatic than on CV1 cells. Therefore, the rate of RNA packaging in VP1-102 infections appears to be diminished in both CV1 and HeLa

TABLE 4. Interference in single-cycle infections[a]

Infection no.	Virus(es)	MOI (PFU/cell)	Titer after 5 h at 39.5°C (10^6 PFU/ml)	HeLa/CV1 plaque ratio
1	Wild type	10	2,100 3,200	16
2	Wild type	20	2,500 3,000	16
3	VP1-101	10	480 635	112
4	Wild type, VP1-101	10, 10	3,100 2,100	13
5	VP1-102	10	51 75	106
6	Wild type, VP1-102	10, 10	1,400 1,700	11

[a] See Table 3, footnotes *a* and *b*.

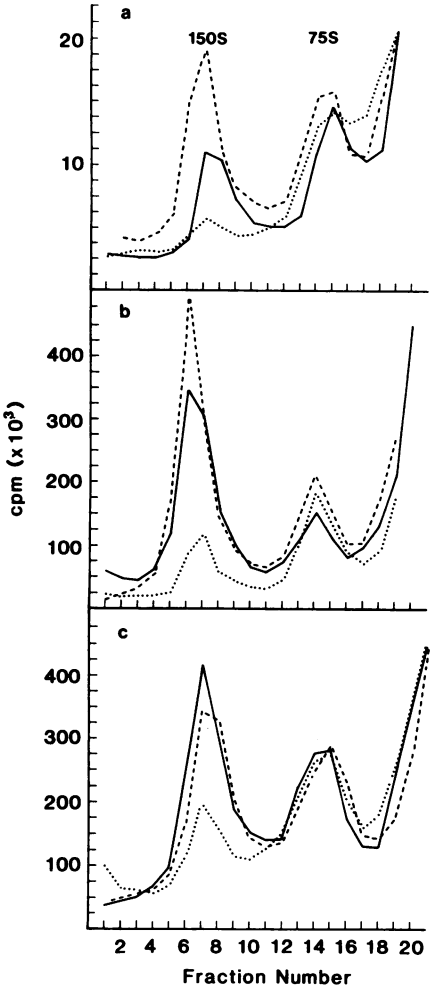

FIG. 6. Viral and subviral particles synthesized during mutant and wild-type infections of CV1 and HeLa cells. ^{35}S-labeled 150S RNA-containing virions and provirions and 75S empty capsids from wild type (——), VP1-101 (– – – –), and VP1-102 (· · · · · ·) are displayed on sucrose gradients. (a) Pattern of particle accumulation on CV1 cells following a 30-min labeling period, from 3 to 3.5 h postinfection. (b) Pattern on CV1 cells following labeling for 90 min, from 3 to 4.5 h postinfection. (c) Particles accumulated in HeLa cells labeled from 3 to 4.5 h postinfection.

cells; this effect may be responsible for the extremely small size of the VP1-102 plaques on both cell lines (Fig. 3), as well as the low virus yield during single-cycle infections.

Phenotypic defects of VP1-101 and VP1-102 result from the mutant proteins, not the RNA. The mutations causing the phenotypes of VP1-101 and VP1-102 map to the region of the RNA genome encoding the amino terminus of VP1 (19). That these mutations are both deletions that preserve the translational reading frame does not argue that the mutations affect only the viral proteins, because any viable virus would need an open reading frame. The possibility exists, therefore, that one or both of these mutants derive their phenotypic defects from the mutation in the viral RNA and that the mutated proteins confer no part of the mutant phenotype.

Complementation analysis can be used to test for the presence of such a *cis*-dominant mutation. Capsid proteins, however, function as a multimer containing 60 copies of each of the structural proteins. Thus, true complementation is not expected, but instead partial dominance or phenotypic mixing, a situation in which the mutant infections are partially complemented by the presence of nonmutant capsid proteins and a wild-type infection is partially poisoned by the presence of the mutant capsid proteins. Depending on the nature and severity of the mutations, these effects are expected to be quite sensitive to the dosage of the mutant and wild-type proteins (26).

The results of a complementation experiment are presented in Table 3. To be able to detect the mutant plaques for subsequent analysis, the coinfecting virus used was 3NC-202, a temperature-sensitive mutant whose defect is in RNA replication and whose capsid proteins are wild type in sequence and function (36). Because 3NC-202 does not replicate at 39.5°C, a high MOI was used to ensure that some nonmutant viral proteins were made from the infecting 3NC-202 RNA.

In infection 1 (Table 3), the numbers of background plaques resulting from the 3NC-202 virus were shown to be quite low. Infections 2 and 3 indicate the yield of wild-type virus and that the yield was neither enhanced nor diminished during coinfection with 3NC-202 virus. Infections 4 and 5 show the yield of VP1-101 during single-cycle infections and that the presence of 3NC-202 virus resulted in a small but reproducible increase in the yield of VP1-101 virus. Furthermore, due to phenotypic mixing, the HeLa/CV1 ratio was significantly diminished in the coinfection between VP1-101 and 3NC-202 virus from its value in the VP1-101 infection alone. Thus, partial complementation of VP1-101 was observed; this complementation affected both the growth rate and the plaquing efficiency of the resulting virus on CV1 and HeLa cells.

Infections 6 and 7 show the low yield of VP1-102 virus in a single-cycle infection and the lack of complementation of VP1-102 during coinfection with 3NC-202. The absence of complementation may be a dosage effect; more nonmutant capsid proteins may be required to rescue a VP1-102 than a VP1-101 virion. If that is true, then VP1-102 proteins should prove more poisonous to a wild-type infection.

In Table 4, the results of an interference experiment are presented. In these experiments, equivalent MOIs of wild-type, VP1-101, and VP1-102 viruses were tested in coinfections for the poisoning of the wild-type infections by the presence of the mutant proteins; this is a test for dominance of the mutants. The yields of both VP1-101 and VP1-102 under the same conditions were less than 20% of the wild-type yields, and therefore the presence of the mutant plaques did not interfere with the analysis of the wild-type yields. Infections 1 and 2 show the comparable yields of wild-type virus from infections initiated at the two different MOIs relevant to the experiment. Lines 3 and 4 display the lack of effect of coinfection with VP1-101 on either the yield of wild-type virus or the resulting HeLa/CV1 ratio. Infections 5 and 6 show, on the other hand, that a significant reduction of the yield of wild-type virus occurred during coinfection with VP1-102. Thus, VP1-102 virus displayed some dominance in a coinfection with wild-type virus. Under similar conditions, VP1-101 showed no dominance over the wild-type infection; this result is consistent with the complementation experiments, in which it seemed possible that fewer copies of nonmutant capsid proteins could complement VP1-101 than would be necessary to complement VP1-102. The model that emerges is that VP1-102 mutant proteins are able to create a mutant phenotype at lower doses than VP1-101 proteins.

The findings that VP1-101 can be complemented and that VP1-102 can show partial dominance confirm the idea that

the mutant capsid proteins contribute to, or are responsible for, the phenotypes of both mutants. The possibility of a direct role for the mutant RNAs in causing the mutant phenotypes is of course not eliminated. However, the simpler idea, that the mutant proteins are solely responsible for the defects in RNA uncoating and encapsidation, is consistent with the data presented here.

DISCUSSION

Two different small deletions in the amino terminus of VP1 of Mahoney serotype 1 poliovirus confer both phenotypic and biochemical defects on the mutant viruses bearing them. Deletion of amino acids 8 and 9, the lesion sustained by mutant VP1-101, had no effect on the binding of the virus to cells or the subsequent conformational alteration of the virion that renders it uninfectious. When time courses of the loss of photoinactivation of wild-type and VP1-101 viruses grown in the presence of neutral red were compared, however, a pronounced delay was observed for VP1-101 (Fig. 5).

The loss of photoinactivation of viruses in which chromogenic dyes are copackaged with the viral RNA presumably measures a structural change that allows the diffusion of dye molecules away from the viral RNA. It has not been clear, however, whether this transition corresponds to physical RNA release or only to conformational alteration of the virion (10, 22). The differences between the time course of the conformational change resulting in loss of infectivity (Fig. 4) and the kinetics of loss of light sensitivity of NR virus (Fig. 5) reported here may help to resolve this uncertainty. The two assays clearly measured different structural transitions, with the transition corresponding to loss of photosensitivity occurring subsequent to the transition corresponding to loss of infectivity. Receptor-dependent loss of viral infectivity has been well correlated with a variety of structural alterations in the virion (10, 22, 34). It seems reasonable to conclude that loss of photosensitivity of NR virus corresponds to the physical uncoating of the viral RNA occurring after the first structural alteration.

Thus, VP1-101 virus displayed delayed RNA release from the mutant viral capsid. The VP1-101 mutation also caused the plaque and growth rate phenotypes of the VP1-101 mutant: fewer and smaller plaques made on CV1 cells in comparison to HeLa cells than wild-type virus, a slightly small-plaque phenotype on HeLa cells, a higher particle/PFU ratio on HeLa cells than wild-type virus, and a fivefold-lower virus yield in single-cycle infections on either HeLa or CV1 cells. That the phenotypic defects of VP1-101 were caused by mutation of the viral protein and not the viral RNA alone was shown by the partial complementation of the VP1-101 phenotype by wild-type capsid proteins (Table 3). Therefore, the small deletion in the amino terminus of VP1 is responsible for both the biochemical defect in RNA release and the phenotypic defects in virus growth. To rationalize the plaque reduction phenotype on CV1 cells, either an increased sensitivity to defects in RNA release for CV1 cells or the direct participation of a cellular component in viral RNA release must be invoked.

Deletion of amino acids 1 to 4 of VP1 of Mahoney serotype 1 poliovirus, the mutation borne by VP1-102, also caused a delay in RNA release mediated by either CV1 or HeLa cells. An additional biochemical defect, in RNA packaging, was discovered for this mutant: the amount of encapsidation of viral RNA, as measured by the relative abundance of RNA-containing and empty viral and subviral particles, was diminished in VP1-102 infections of both CV1 and HeLa cells.

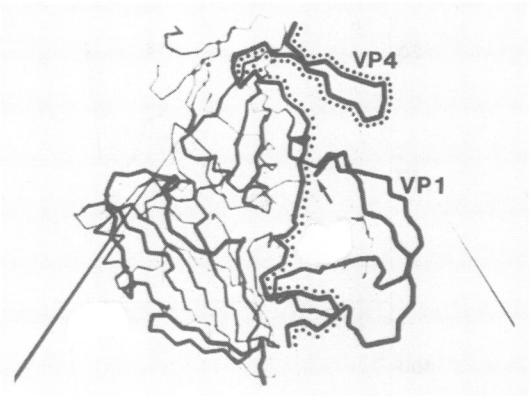

FIG. 7. Diagram of the peptide backbone of the capsid proteins on the inside of the virion, closest to the viral RNA. The most amino-terminal residues of VP1 that were resolved in the three-dimensional structure of poliovirus determined at 2.9 Å resolution are denoted with the arrow. The entire chain of VP4 is marked with adjacent dots. (From J. Hogle et al. [17]; used with permission.)

The VP1-102 mutation also caused the phenotype of the VP1-102 mutant virus: very small plaques on both CV1 and HeLa cells, a 50-fold decrease in virus titer in single-cycle infections of either cell line, a reduction in the relative numbers of plaques on CV1 cells, and a higher particle/PFU ratio than wild-type virus prepared under the same conditions. Some aspect of the mutant phenotype was caused by the defective VP1-102 protein alone, because VP1-102 virus displayed partial dominance during coinfection with wild-type virus (Table 4). The VP1-102 mutations is thus responsible both for biochemical defects in RNA release from the virion and RNA packaging and for the phenotypic defects discussed above.

These two different alleles of VP1 demonstrate, therefore, that RNA packaging into viral particles and RNA release from viral particles are related but separable genetic functions. Somehow, the amino terminus of VP1 is intimately involved in both these functions. Recent refinement of the three-dimensional structure of Mahoney serotype 1 poliovirus has revealed the locations of a few of the most amino-terminal residues of VP1 (14). Figure 7 presents a view from the inside of the viral particle of the network formed by VP4 and the amino-terminal extensions of VP1, VP2, and VP3 (17). An arrow denotes residue 20 of VP1; the more amino-terminal residues are not shown in this diagram, but density corresponding to several of them comprises a third beta-strand, hydrogen bonded to VP4 near the fivefold symmetry axis (14).

During the cell-mediated structural alteration of poliovirions that results in loss of elutable, infectious virus, VP4 is lost from the viral capsid (10), and the resulting particles become more lipophilic (21). The amino terminus of VP4 has been shown to be myristylated in intact virions (8); the presence of this hydrophobic moiety may facilitate the structural transition. Subsequent to structural alteration, the slightly hydrophobic amino termini of VP1 become more sensitive to proteolysis, a change thought to correspond to an extrusion of these portions of VP1 (14). I have shown here that the cell-mediated structural changes leading to loss of viral infectivity are unaffected by small deletions in the amino terminus of VP1. Less is known about the subsequent change in the virion leading to RNA release; this process is critically affected, however, by the small deletions in the VP1-101 and VP1-102 mutants.

If RNA encapsidation were the microscopic reverse of RNA release, it would be expected that mutants demonstrating slower release of RNA might display more rapid RNA packaging. While this may be the case for VP1-101, it certainly is not for VP1-102, which shows delayed kinetics for both processes (Fig. 5 and 6). That the two processes show some genetic and perhaps mechanistic features, however, was suggested by their simultaneous impairment in the VP1-102 mutant.

Several picornavirus mutants defective in various stages of entry into cells have been sequenced, and some have been characterized by reconstruction to substantiate that the detected lesion is responsible for the mutant phenotype. Targeted mutations were constructed in the proposed receptor-binding site of human rhinovirus type 14 (9); several of the resulting mutants were specifically defective in binding to susceptible cells, supporting the idea that the deep indentation or canyon encircling the five-fold symmetry axis of rhinovirus is the receptor-binding site (9, 33). Replacement of six amino acids in VP1 of Mahoney serotype 1 poliovirions with amino acids from a similar position in Lansing serotype 2 poliovirions resulted in the simultaneous transfer of the Lansing phenotype of neurovirulence in mice (27). This effect may have resulted from the acquisition by the hybrid virus of the ability to bind to mouse receptors (27). The changed residues are located in a loop near the fivefold symmetry axis of the particles, neighboring but not constituting the proposed receptor-binding site (33). The three-dimensional structure of a human rhinovirus 14 variant that is resistant to inhibition by certain antiviral compounds has been determined, and a mutation has been found within the drug-binding site (2). In the present work, two defined Mahoney serotype 1 poliovirus mutants have been described that carry mutations that specifically affect a later stage of virus entry into cells, the physical release of the viral RNA from the capsid. An unexpected connection between RNA release and RNA encapsidation was shown by the concomitant defects in both these processes in one of the mutants. The location of the responsible mutations in the amino terminus of VP1 suggests a direct role for these sequences in viral RNA manipulation during cell entry and virion morphogenesis of wild-type poliovirions.

ACKNOWLEDGMENTS

I thank Jim Hogle for provision of unpublished results and permission to use images of the three-dimensional structure of poliovirus and Peter Sarnow for numerous suggestions during the course of the experiments and the gift of the T7D plasmid. I am grateful to David Baltimore, Robert Boswell, Minx Fuller, Connie Nugent, Peter Russell, and Peter Sarnow for helpful comments on the manuscript.

This work was supported by Public Health Service grant AI-25166 from the National Institutes of Health, Junior Faculty Award JFRA-171 from the American Cancer Society, and the Searle Scholar's Fund.

LITERATURE CITED

1. **Arnold, E., M. Luo, G. Vriend, M. G. Rossmann, A. C. Palmenberg, G. D. Parks, M. J. H. Nicklin, and E. Wimmer.** 1987. Implications of the picornavirus capsid structure for polyprotein processing. Proc. Natl. Acad. Sci. USA **84**:21–25.
2. **Badger, J., I. Minor, M. J. Kremer, M. A. Oliveira, T. J. Smith, J. P. Giffith, D. M. A. Guerin, S. Krishnaswamy, M. Luo, M. G. Rossman, M. A. McKinlay, G. D. Diana, F. J. Dutko, M. Fancher, R. R. Rueckert, and B. A. Heinz.** 1988. Structural analysis of a series of antiviral agents complexed with human rhinovirus 14. Proc. Natl. Acad. Sci. USA **85**:3304–3308.
3. **Baltimore, D.** 1985. Picornaviruses are no longer black boxes. Science **229**:1366–1367.
4. **Baltimore, D., M. Girard, and J. E. Darnell.** 1966. Aspects of the synthesis of poliovirus RNA and the formation of virus particles. Virology **29**:179–189.
5. **Baron, M. H., and D. Baltimore.** 1982. Antibodies against the chemically synthesized genome-linked protein of poliovirus react with native virus-specific proteins. Cell **28**:395–404.
6. **Bernstein, H. D., N. Sonenberg, and D. Baltimore.** 1985. Poliovirus mutant that does not selectively inhibit host cell protein synthesis. Mol. Cell. Biol. **5**:2913–2923.
7. **Caliguiri, L. A., J. J. McSharry, and G. W. Lawrence.** 1980. Effect of arildone on modifications of polivirus *in vitro*. Virology **97**:86–93.
8. **Chow, M., J. F. E. Newman, D. Filman, J. M. Hogle, D. J. Rowlands, and F. Brown.** 1987. Myristylation of picornavirus capsid protein VP4 and its structural significance. Nature (London) **327**:482–486.
9. **Colonno, R. J., J. H. Condra, S. Mizutani, P. L. Callahan, M. Davies, and M. A. Murcko.** 1988. Evidence for the direct involvement of the rhinovirus canyon in receptor binding. Proc. Natl. Acad. Sci. USA **85**:5449–5453.
10. **Crowell, R. L., and B. J. Landau.** 1983. Receptors in the initiation of picornavirus infections, p. 1–41. *In* H. Fraenkel-Conrat and R. R. Wagner (ed.), Comprehensive virology. Plenum Publishing Corp., New York.
11. **Crowther, D., and J. L. Melnick.** 1962. The incorporation of neutral red and acridine orange into developing poliovirus particles making them photosensitive. Virology **14**:11–21.
12. **de Sena, J., and B. Mandel.** 1977. Studies on the *in vitro* uncoating of poliovirus. Virology **78**:554–566.
13. **Eggers, H. J.** 1977. Selective inhibition of uncoating of echovirus 12 by rhodanine. Virology **78**:241–252.
14. **Filman, D. J., R. Syed, M. Chow, A. J. Macadam, P. D. Minor, and J. M. Hogle.** 1989. Structural factors that control conformational transitions and serotype specificity in type 3 poliovirus. EMBO J. **8**:1567–1579.
15. **Greve, J. M., G. Davis, A. M. Meyer, C. P. Forte, S. C. Yost, C. W. Marlor, M. E. Kararck, and A. McClelland.** 1989. The major human rhinovirus receptor is ICAM-1. Cell **56**:839–847.
16. **Guttman, N., and D. Baltimore.** 1977. A plasma membrane component able to bind and alter virions of poliovirus type 1: studies of cell-free alteration using a simplified assay. Virology **82**:25–36.
17. **Hogle, J. M., M. Chow, and D. F. Filman.** 1985. Three-dimensional structure of poliovirus at 2.9 Å resolution. Science **229**:1358–1365.
18. **Holland, J. J.** 1962. Irreversible eclipse of poliovirus by HeLa cells. Virology **16**:163–176.
19. **Kirkegaard, K., and B. Nelsen.** 1990. Conditional poliovirus mutants made by random deletion mutagenesis of infectious cDNA. J. Virol. **64**:185–194.
20. **Kitamura, N., B. Semler, P. Rothberg, G. Larsen, C. Adler, A. Dorner, E. Emini, R. Hanecak, J. Lee, S. van der Werf, C. Anderson, and E. Wimmer.** 1981. Primary structure, gene organisation, and polypeptide expression of poliovirus RNA. Nature (London) **291**:547–553.
21. **Lonberg-Holm, K., L. B. Gosser, and E. J. Shimshick.** 1976. Interaction of liposomes with subviral particles of poliovirus type 2 and rhinovirus type 2. J. Virol. **19**:746–749.
22. **Madshus, I. H., S. Olsnes, and K. Sandvig.** 1984. Mechanism of entry into the cytosol of poliovirus type 1: requirement for low pH. J. Cell Biol. **98**:1194–1200.
23. **Mandel, B.** 1985. The fate of the inoculum in HeLa cells infected with poliovirus. Virology **25**:152–154.
24. **McSharry, J. J., L. A. Caliguiri, and H. J. Eggers.** 1979. Inhibition of uncoating of poliovirus by arildone, a new antiviral drug. Virology **97**:307–315.
25. **Mendelsohn, C. L., E. Wimmer, and V. R. Racaniello.** 1989. Cellular receptor for poliovirus: molecular cloning, nucleotide sequence, and expression of a new member of the immunoglobulin superfamily. Cell **56**:855–865.
26. **Muller, H. J.** 1932. Further studies on the nature and causes of

gene mutations. Sixth Int. Cong. Genet. **1**:213–255.
27. **Murray, M. G., J. Bradley, X. F. Yang, E. Wimmer, E. G. Moss, and V. R. Racaniello.** 1988. Poliovirus host range is determined by a short amino acid sequence in neutralization antigenic site I. Science **242**:213–215.
28. **Neubauer, C., L. Frasel, E. Kuechler, and D. Blaas.** 1987. Mechanism of entry of human rhinovirus 2 into HeLa cells. Virology **158**:255–258.
29. **Ninomiya, Y., C. Ohsawa, M. Aoyama, I. Umeda, Y. Suhara, and H. Ishitsuka.** 1984. Antivirus agent Ro 09-0410 binds to rhinovirus specifically and stabilizes the virus conformation. Virology **134**:269–276.
30. **Putnak, J. R., and B. A. Phillips.** 1981. Picornaviral structure and assembly. Microbiol. Rev. **45**:287–315.
31. **Racaniello, V. R., and D. Baltimore.** 1981. Cloned poliovirus complementary DNA is infectious in mammalian cells. Science **214**:916–919.
32. **Racaniello, V. R., and D. Baltimore.** 1981. Molecular cloning of poliovirus cDNA and determination of the complete nucleotide sequence of the viral genome. Proc. Natl. Acad. Sci. USA **78**:4887–4891.
33. **Rossman, M. G., E. Arnold, J. W. Erickson, E. A. Frankenberger, J. P. Griffith, H. J. Hecht, J. E. Johnson, G. Kamer, M. Luo, A. G. Mosser, R. R. Rueckert, B. Sherry, and G. Vriend.** 1985. Structure of a human common cold virus and functional relationship to other picornaviruses. Nature (London) **317**: 145–153.
34. **Rueckert, R. R.** 1986. Picornaviruses and their replication, p. 357–390. *In* B. N. Fields and D. M. Knipe (ed.), Fundamental virology. Raven Press, New York.
35. **Sarnow, P.** 1989. Role of 3′-end sequences in infectivity of poliovirus transcripts made in vitro. J. Virol. **63**:467–470.
36. **Sarnow, P., H. D. Bernstein, and D. Baltimore.** 1986. A poliovirus temperature-sensitive RNA synthesis mutant located in a noncoding region of the genome. Proc. Natl. Acad. Sci. USA **83**:571–575.
37. **Smith, T. J., M. J. Kremer, M. Luo, G. Vriend, E. Arnold, G. Kamer, M. G. Rossmann, M. A. McKinlay, G. D. Diana, and M. J. Otto.** 1986. The site of attachment in human rhinovirus 14 for antiviral agents that inhibit uncoating. Science **233**:1286–1293.
38. **Staunton, D. E., V. J. Merluzzi, R. Rothlen, R. Barton, S. D. Marlin, and T. A. Springer.** 1989. A cell adhesion molecule, ICAM-1, is the major surface receptor for rhinoviruses. Cell **56**:849–853.
39. **van der Werf, S., J. Bradley, E. Simmer, F. Studier, and J. Dunn.** 1986. Synthesis of infectious poliovirus RNA by purified T7 RNA polymerase. Proc. Natl. Acad. Sci. USA **83**:2330–2334.
40. **Wilson, J. N., and P. D. Cooper.** 1963. Aspects of the growth of poliovirus as revealed by the photodynamic effects of neutral red and acridine orange. Virology **21**:135–145.
41. **Zeichhardt, H., M. J. Otto, M. A. McKinlay, P. Willingmann, and K. O. Habermehl.** 1987. Inhibition of poliovirus uncoating by disoxaril (WIN 51711). Virology **160**:281–285.